Optics Communications 282 (2009) 3168–3171

Contents lists available at ScienceDirect

Optics Communications

journal homepage: www.elsevier.com/locate/optcom

Integrated photonic crystal spectrometers for sensing applications

Babak Momeni *, Ehsan Shah Hosseini, Murtaza Askari, Mohammad Soltani, Ali Adibi

School of Electrical and Computer Engineering, Georgia Institute of Technology, Atlanta, GA 30332, USA

ARTICLE INFO

Article history:
Received 15 December 2008
Received in revised form 12 March 2009
Accepted 21 April 2009

ABSTRACT

A combination of negative refraction and diffraction compensation in a superprism-based photonic crystal structure is used to demonstrate a compact on-chip photonic crystal spectrometer. This structure provides strong dispersion and signal isolation, which are essential for forming an efficient and compact spectrometer. Performance of these spectrometers as spectral pattern detectors is discussed. The experimental results show that a PC structure with 80 μm × 220 μm dimension can locate a single spectral feature with better than 10 pm accuracy over a bandwidth of 50 nm around 1550 nm center wavelength at an output signal-to-noise ratio of 13 dB.

© 2009 Elsevier B.V. All rights reserved.

1. Introduction

Integrated optical sensors in different material platforms have attracted considerable research activities recently due to their potentials to perform chemical and biological sensing, particularly in lab-on-a-chip applications. The main advantage of integrated sensors is their compactness, which enables their operation with only a small amount of specimen. This advantage, when combined with sensitive optical probing techniques, provides a potentially large sensitivity obtained through field enhancement in a non-invasive or minimally invasive approach. Furthermore, the possibility of integrating photonic and electronic functionalities on a single substrate (e.g., silicon) allows for the entire sensing module to be implemented in a very small microchip. Fig. 1 shows the schematics of a lab-on-a-chip sensing module with light–matter interaction in a resonator followed by spectral analysis, detection, and electronic processing.

Among different possible detection schemes for integrated optical sensors, spectral analysis enables versatile sensing mechanisms such as those based on absorption [1], fluorescence [2], or Raman effects [3]. These implementations require a spectrometry step, which is typically performed using off-chip detection mechanisms [4] or stand-alone off-chip spectrometers [5,6]. These off-chip techniques degrade the overall detection performance and increase the overall device size, and thus, take away the advantages of having a compact sensor. These issues are resolved using an integrated on-chip spectrometer.

Different approaches have been proposed to implement on-chip spectrometers in an integrated optical platform [7,8]. Despite impressive progress in recent years, several challenges must still be addressed before such spectrometers can be used in practical lab-on-a-chip systems. These challenges include overall size (i.e., compactness), material compatibility in an integrated platform, and meeting the required resolution demand for practical applications. In this paper, we demonstrate a new solution for practical on-chip spectrometers that are applicable to a wide range of sensing mechanisms by addressing the major challenges discussed above. The proposed spectrometers are enabled by dispersion engineering in photonic crystals (PCs) using a recently demonstrated demultiplexing concept [9]. The motivations behind choosing PCs as the platform for the spectrometer are their strong dispersive properties that can result in a high spectral resolution (even within a small footprint) and their compatibility with an integrated optical platform, which makes it possible to combine it with other sensing and optical processing stages. We show that the accuracy of these PC spectrometers in detecting sharp spectral features meets the requirements for current sensing applications in a compact and integrated platform, while their size is considerably smaller than other existing alternatives.

2. Spectrometer demonstration

There are two basic conditions needed to realize an effective spectrometer: first, the optical device needs to provide a mapping from spectrum to space with enough diversity to allow for accurate estimation of the spectrum of an unknown input signal. Second, it needs to efficiently isolate the signal at the output from stray light and unwanted contributions. Three unique dispersive properties of PCs can be used simultaneously to achieve these conditions: by combining superprism effect [10] and diffraction compensation [11], it is possible to spatially separate different frequencies in a compact structure [12]. Additionally, by designing the structure in the negative refraction regime [13], we can isolate the signal of interest from stray light and unwanted contributions (e.g.,

* Corresponding author. Tel.: +1 404 385 4201.
E-mail addresses: bmomeni@gatech.edu, momeni@ece.gatech.edu (B. Momeni).

0030-4018/$ - see front matter © 2009 Elsevier B.V. All rights reserved.
doi:10.1016/j.optcom.2009.04.052

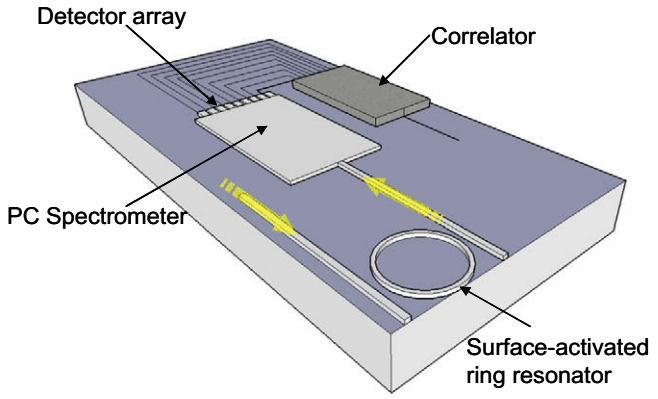

Fig. 1. Suggested configuration for the implementation of an integrated spectrometer for sensing applications is shown. The role of the spectrometer in this system is to detect the changes induced in the spectrum of the optical resonator by the attachment of the analyte to its surface.

power in unwanted polarizations or out-of-band frequencies) [9]. The operation principle of the proposed spectrometers is schematically shown in Fig. 2a. Input signals at different wavelengths are separated in angle upon entering the PC because of the superprism effect. The signals at different wavelengths then get focused while propagating inside the PC through the negative diffraction effect. The desired signals are also refracted in the negative refraction regime and are separated from the stray light. The simultaneous presence of these three dispersive properties results in a diverse spectral–spatial mapping in a very compact structure to form a powerful on-chip spectrometer. The output of the PC device is sampled by an array of waveguides as shown in Fig. 2a for final detection and subsequent spectrum estimation.

While the concept shown in Fig. 2a is applicable for designing both PC wavelength demultiplexers and PC spectrometers, the design criteria for these two applications are different. The main goal in PC wavelength demultiplexers is the complete separation of the input wavelength channels with minimal cross-talk and high resolution (i.e., very small wavelength spacing between adjacent channels) [14]. On the other hand, the ultimate goal in the design of PC spectrometers for sensing applications is to accurately detect spectral features (e.g., Raman peaks or very small shifts in the resonance frequency of a resonator) in the presence of noise [15]. To achieve this goal, the design parameters of the PC structure must be optimized for maximal spatial–spectral diversity at low insertion losses. By following a direct optimization process, we have designed a PC structure for on-chip spectroscopy in the form of a square lattice of air holes in a planar silicon-on-insulator (SOI) platform. The structure has been fabricated on a SOI substrate using electron-beam lithography and dry etching as outlined in Ref. [9]. The scanning electron microscopy (SEM) images of the fabricated structure are shown in Fig. 2b, revealing the details of the structure at the input interface and the array of output waveguides. The structure is a 45°-rotated square lattice and has a normalized radius of holes $r/a = 0.30$, with $a = 370$ nm being the lattice constant. The thickness of the Si device layer in the final structure is 230 nm ± 10 nm. The incident beam has a TE-like polarization (i.e., its electric field is primarily in the plane of periodicity of the PC structure) and illuminates the PC structure at an incident angle of 15°. The entire size of the PC structure in this spectrometer is 80 μm × 220 μm.

To test the performance of the fabricated PC spectrometer, the input light from a tunable laser source (Agilent 81640A) is focused by a microscope objective lens (40×) onto the input waveguide, which carries the light to the PC structure. At the output of the PC spectrometer, the light from the waveguide array (see Fig. 2b) is imaged onto an infrared camera to measure the spatial distribution of the output light. The laser wavelength is swept in steps of 0.025 nm over 50 nm (i.e., 1560–1610 nm), and the output pattern is measured at each wavelength to obtain the spatial–spectral mapping of the PC spectrometer. The relative wavelength accuracy of the tunable laser used in our measurements is ±3 pm, and its linewidth is 100 kHz; therefore, we expect minimal inaccuracies induced by the laser source in our measurement results.

Fig. 3 shows the experimentally measured spatial–spectral mapping (i.e., the distribution of power in the output waveguide array at different wavelengths) for the PC spectrometer shown in Fig. 2b. Each vertical line in Fig. 3 corresponds to a single input wavelength, and the power in 24 output waveguides is measured. Alternatively, each row in Fig. 3 shows the output of one of the waveguides at different wavelengths. For clarity of presentation, only a subset of the measured data at 1 nm wavelength spacing (instead of the actual 0.025 nm spacing) is shown. The wavelength-dependent beam steering caused by the superprism effect is evident from Fig. 3. It is also clear that the PC spectrometer does not provide complete separation of the adjacent wavelength channels (in contrast to what is expected from a wavelength demultiplexer). In fact, to optimize the spectral estimation process, the device is designed to have around 3 dB cross-talk between adjacent channels (which corresponds to the Nyquist rate for the spatial sampling of the optical beam at the output of the photonic crystal region).

Note that our PC spectrometers are designed to accurately detect individual spectral features (e.g., resonator peaks or Raman

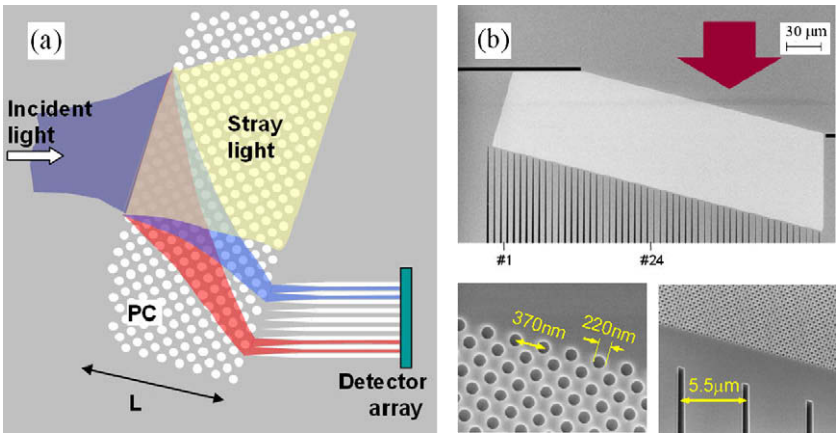

Fig. 2. (a) Schematic of the operating principle of the fabricated PC spectrometer, which combines three dispersive properties of PCs. (b) Scanning electron microscopy (SEM) image of the PC structure with insets showing details of the interface of the PC and the array of waveguides that sample the optical beam at the output of the PC region.

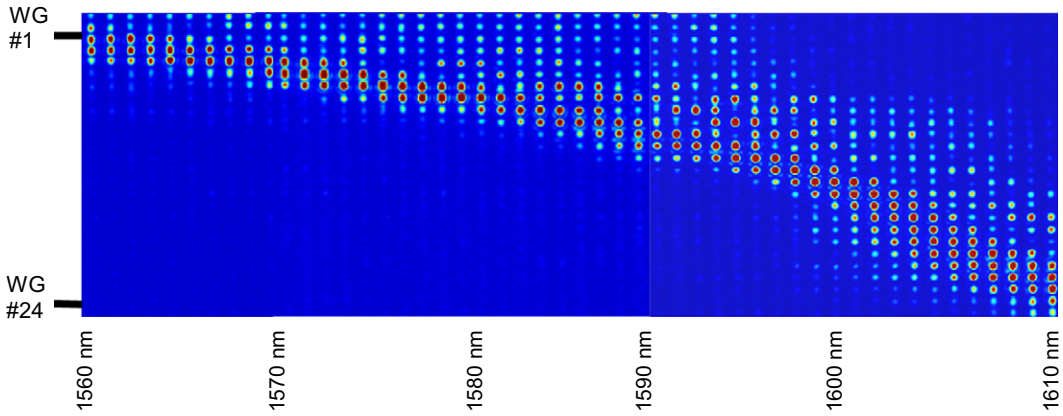

Fig. 3. Power distributions at different output waveguides over a 50 nm bandwidth are shown. Each row corresponds to one output waveguide, and each column shows the power distribution at a specific wavelength.

spectrum). They are not intended as general-purpose spectrometers to detect an analog spectrum over a wide wavelength range. In this context, the 50 nm operation bandwidth of the designed PC spectrometer provides enough dynamic range for most practical applications of these spectrometers (e.g., multiplexing ~10 resonators in a multiplexed sensor for refractive index monitoring, or analyzing the typical Raman spectra [16]).

In a typical lab-on-a-chip sensing module (shown in Fig. 1), the attachment of the analyte of interest to the surface of a resonator results in a small shift in the resonance frequency. Since sensing schemes rely on detecting very small amounts of the target analyte, the key feature expected from the on-chip spectrometer is to detect such small changes in resonance features. To assess the performance of our PC spectrometer in such configurations, we use the calibration data (found experimentally, as discussed above) to estimate the wavelength of an incoming spectral peak at an unknown wavelength, in the presence of noise. To extract the location of each spectral peak (i.e., the input wavelength), we use a maximum likelihood criterion by correlating the set of measured powers in the output waveguides for the unknown input with all the calibration data. The wavelength with the maximum correlation factor is the estimated wavelength for the input signal. To find the estimation error for different levels of noise, we have used a statistical analysis based on the experimentally measured response

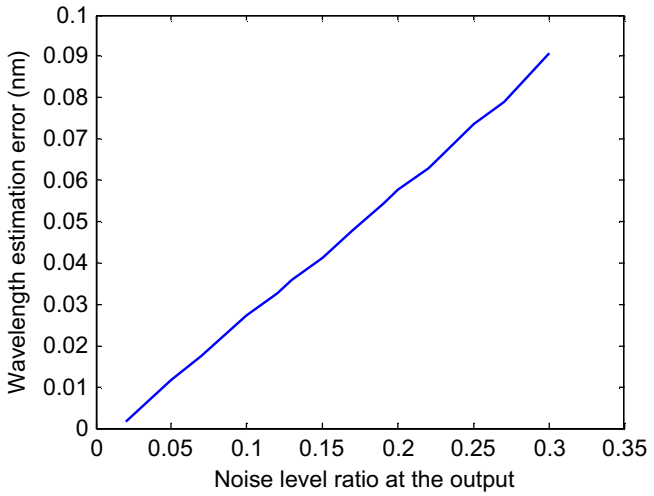

Fig. 4. The response of the PC spectrometer for estimating the location of a spectral peak (based on the experimental characterization of the device) is shown. The estimation error is defined as the average error in locating the input wavelength calculated for a set of input signals that are randomly distributed in wavelength.

of the system and by modeling the noise in the simulations. We consider the collective effect of noise from different sources in the system as an additive Gaussian noise at the detection stage. The statistical analysis of the noise is then performed by adding the Gaussian noise (in software) to the output of the spectrometer for a known input (i.e., a randomly picked sample from the calibration data). The noise-degraded output is then compared with the calibration data (i.e., experimentally obtained response of the system), and the difference between the actual wavelength of the input signal and the estimated wavelength is obtained from a maximum likelihood criterion. This procedure is repeated multiple times (for 100 different input signals and 50 different samples of noise for each input), and a statistical ensemble is formed. The mean estimation error of that ensemble at each noise level is reported in Fig. 4. We have repeated this procedure for different wavelength spacing of the calibration data, and in all cases the results have been consistent with the plot shown in Fig. 4.

Fig. 4 shows that our PC spectrometer can detect single spectral features with high accuracy under reasonable signal-to-noise ratios (SNRs). For example, even at a relatively low $(SNR)_o = 13$ dB (i.e., noise to signal ratio of 0.05 at the detector), the spectral location of a single peak is detected with better than 10 pm accuracy. This 10 pm accuracy at the modest $(SNR)_o$ of 13 dB enables the detection of refractive index change of the order of 10^{-4}–10^{-5} in the sensing device shown in Fig. 1. Note that there is an inverse relation between the estimation error and the $(SNR)_o$; therefore, much better values of wavelength accuracy are achievable at higher $(SNR)_o$ values (readily accessible in a practical sensing module, using the currently available LED sources and photodetectors). It is more remarkable to note that the size of the PC device is only 80 μm × 220 μm, which enables compact integration of the spectral analysis module with the transducer components. The ability of the PC spectrometer to determine the wavelength of a spectral peak with such high accuracy lies in the fact that we are using all the available information obtained from the device to extract a single parameter (the center wavelength of the spectral peak). In other sensing schemes, several spectral features may be present in the output spectrum (e.g., in a Raman signal), and estimating the location of all the features can be performed in the same manner. Clearly, the accuracy of the device might be reduced as the amount of information to be extracted increases. However, if there is enough wavelength separation between the spectral features (around 8 nm for the structure shown in Fig. 2), the reduction in the accuracy of the device can be minimized. As an example, typical Raman spectra of interest in biosensing applications include Raman peaks that are 10–20 nm apart [16]. This also suggests that the PC spectrometer can be used to detect multiple analytes on the same chip

if a multiplexed sensing architecture is employed (e.g., by assigning one resonator for each analyte using the structure shown in Fig. 1, with resonance wavelengths separated by a few nm).

The amount of information at the PC spectrometer output (and therefore, the accuracy of the device) can be further improved by increasing the SNR of the measurement. By using integrated sources and detectors, a lock-in detection scheme, and longer integration times, we expect to significantly reduce the noise in this device, which will result in better resolution. Another important consideration is that the detection of spatial diversity in planar integrated spectrometers is limited to a one-dimensional distribution in a linear array of output detectors. This limitation significantly reduces the amount of spatial information that could be resolved with a two-dimensional array as found in many bulk spectrometers. Nevertheless, using a strongly dispersive PC structure, as shown in this paper, it is possible to partially compensate these effects and realize a compact PC spectrometer with a resolution that meets the requirements of current sensing applications.

The insertion loss of the current PC spectrometer is around 8 dB (compared to a straight waveguide on the same wafer). We think the insertion loss can be considerably reduced by optimizing the input and output waveguide feeds to reduce coupling losses, and by using proper matching stages to reduce reflection and scattering losses at the interfaces of the PC region. Improvements in the fabrication quality will also reduce the propagation loss through the PC structure. Compared to other techniques for the development of on-chip spectrometers, the key advantage of the proposed PC spectrometers is the design flexibility through PC dispersion engineering. This allows us to realize the most compact structure for a given performance measure. Reaching spectral resolution and detection accuracies needed in sensing application in such a small footprint ($\sim$100 μm dimension) makes it possible to implement a variety of new sensing schemes and mechanisms on chip. Thus, we believe that these PC spectrometers with further optimization have the potential to revolutionize the field of on-chip sensing by enabling ultracompact functional lab-on-a-chip modules with spectral analysis capabilities.

3. Conclusion

In conclusion, we have demonstrated an integrated optical spectrometer that utilizes the unique dispersive properties of photonic crystals. We have shown that these spectrometers can be optimally engineered to detect spectral features in an integrated sensing platform with high accuracy despite having a very small size. Our results indicate an ability to locate a spectral peak with better than 10 pm wavelength accuracy over a 50 nm bandwidth at an output SNR of 13 dB. With further optimization of the device and its fabrication (e.g., by using strongly dispersive PCs [17], and improving the input/output coupling efficiencies), we expect to achieve more compact spectrometers with better wavelength estimation accuracy at acceptable insertion losses.

Acknowledgment

This work was supported by Air Force Office of Scientific Research under Contract No. F49620-03-1-0362 (G. Pomrenke) and by National Science Foundation under Contract No. ECS-0239355. The authors would like to thank Charles H. Camp Jr. for useful discussions.

References

[1] D. Richter, D.G. Lancaster, F.K. Tittel, Appl. Opt. 39 (2000) 4444.
[2] R.J. McNichols, G.L. Cote, J. Biomed. Opt. 5 (2000) 5.
[3] T. Vo-Dinh, Sens. Actuat. B 29 (1995) 183.
[4] I. Stemmler, A. Brecht, G. Gauglitz, Sens. Actuat. B 54 (1999) 98.
[5] D.H. Luo, R.A. Levy, Y.F. Hor, J.F. Federici, R.M. Pafchek, Sens. Actuat. B 92 (2003) 121.
[6] P. Niewczas, L. Dziuda, G. Fusiek, A.J. Willshire, J.R. McDonald, G. Thursby, D. Harvey, W.C. Michie, IEEE Trans. Instrum. Meas. 52 (2003) 1092.
[7] P.C. Clemens, G. Heise, R. Marz, H. Michel, A. Reichelt, H.W. Schneider, IEEE Photon. Technol. Lett. 6 (2004) 1109.
[8] R.F. Wolffenbuttel, IEEE Trans. Instrum. Meas. 53 (2004) 197.
[9] B. Momeni, J. Huang, M. Soltani, M. Askari, S. Mohammadi, M. Rakhshandehroo, A. Adibi, Opt. Express 14 (2006) 2413.
[10] H. Kosaka, T. Kawashima, A. Tomita, M. Notomi, T. Tamamura, T. Sato, S. Kawakami, J. Lightwave Technol. 17 (1999) 2032.
[11] B. Momeni, A. Adibi, J. Lightwave Technol. 23 (2005) 1522.
[12] B. Momeni, A. Adibi, Appl. Opt. 45 (2006) 8466.
[13] M. Notomi, Phys. Rev. B 62 (2000) 10696.
[14] K. Okamoto, H. Yamada, Opt. Lett. 20 (1995) 43.
[15] B. Momeni, E. Shah Hosseini, M. Askari, S. Mohammadi, M. Soltani, A. Adibi, Proc. SPIE 6480 (2007) 648012.
[16] S. Shanmukh, L. Jones, J. Driskell, Y. Zhao, R. Dluhy, R.A. Tripp, Nano Lett. 6 (2006) 2630.
[17] B. Momeni, M. Chamanzar, E. Shah Hosseini, M. Askari, M. Soltani, A. Adibi, Opt. Express 16 (2008) 14213.